JOURNAL OF CATALYSIS 152, 341–349 (1995)

Acidic Properties of Sulfated Zirconia: An Infrared Spectroscopic Study

Frédéric Babou, Gisèle Coudurier, and Jacques C. Vedrine[1]

Institut de Recherches sur la Catalyse (CNRS), 2 Avenue Albert Einstein, F-69626 Villeurbanne Cedex, France

Received August 26, 1994; revised November 7, 1994

Sulfated zirconia with S content of 2 wt.% equivalent to complete coverage of its surface was studied by infrared spectroscopy. At least four sulfated species were identified and exhibited an important and reversible sensitivity to water as schematized below:

$$(SO_3)_{ads} + H_2O \leftrightharpoons (H_2SO_4)_{ads}$$

$$(H_2SO_4)_{ads} + 2(H_2O)_{ads} \leftrightharpoons (H_3O^+)_{ads} + (HSO_4^-)_{ads}$$

$$+ (H_2O)_{ads} \leftrightharpoons 2(H_3O^+)_{ads} + (SO_4^{2-})_{ads}.$$

These equilibria were demonstrated to exist by the study of adsorption of incremental amounts of water. D_2O and $H_2{}^{18}O$ isotopically enriched water molecules were used to assist interpretation of IR spectra. To characterize acidity features, the probe molecules butane, CO, and H_2O (as weak bases) or pyridine (as a strong base) were adsorbed. Two Lewis acid sites (L_1 and L_2) were observed and one Brønsted site (B) related to the zirconia support (L_1) and the sulfated species (L_2, B). They were evidenced by pyridine adsorption which was shown to partly displace adsorbed sulfate species. With the help of previous theoretical calculations using an ab initio method and representing the zirconia surface by a mononuclear zirconium complex, it is emphasized that the sulfated zirconia can be visualized as a H_2SO_4 compound grafted onto the surface of zirconia in a way which makes it very sensitive to water but in a reversible way. Its acidity is similar to that of sulfuric acid but it is not really superacidic. Comparison with other oxides leads us to suggest that the cationic charge borne by the metallic cation is of prime importance for the acidity strength. The role of water on the acidic and catalytic properties for *n*-butane isomerization reaction is emphasized. © 1995 Academic Press, Inc.

I. INTRODUCTION

Skeletal isomerization of *n*-alkanes and alkylation of aliphatics by olefins in acid catalysis are important reactions for future reformulated gasoline. Such a gasoline formulation as defined by environmental protection agencies is expected to be effective in 1997 in the United States and later on in Japan and in Europe. In particular the branched A_8 aromatics are expected to be allowed in only limited amounts and will need to be replaced by C_8 branched aliphatics such as trimethylpentanes. Moreover, butane is the major component of the C_4–C_5 cuts in petroleum refineries and is already upgraded by its isomerization into isobutane which may be either transformed into isobutene as a precursor for methyl *tert*-butyl ether (MTBE) or alkylated by butene into trimethylpentanes.

At present this isomerization is performed industrially on a Pt on chlorinated alumina catalyst, while for the aliphatic alkylation reaction HF or H_2SO_4 are used as catalysts (1–3). The replacement of chlorinated alumina, which necessitates the continuous feeding of a chloride compound such as CCl_4 during reaction to maintain its activity, appears to be necessary in the future for environment protection. Solid acidic catalysts seem to be the key to the problem. Some of them are already well known, e.g., silica–aluminas, zeolites, aluminium phosphates, heteropolyacids, resins (Amberlyst, Nafion). Recently a new family of materials, sulfated oxides, particularly zirconia, has been introduced by Japanese researchers (4–9). Much work has already been devoted to sulfated oxides and sulfated zirconia is considered to be a superacid, i.e., having an acid strength higher than that of 100% H_2SO_4. In previous work (10–12) we have shown how to synthesize the best sulfated zirconia without additives; i.e., we have described the best preparation conditions. In addition, quantum chemistry ab initio calculations have been carried out (13) representing zirconium hydroxide by a molecular cluster of limited size. The calculation using H_2O and CO molecules to probe the acid strength has shown that the sulfated zirconia corresponds to H_2SO_4 grafted onto zirconia surface with an acidity close to that of pure H_2SO_4, i.e., strong but not really superacid.

In the present work we have tried to characterize the acid feature of sulfated zirconia using the same approach as described above (H_2O and CO as probing molecules) but with the help of infrared spectroscopy.

[1] To whom correspondence should be addressed.

0021-9517/95 $6.00

II. EXPERIMENTAL

1. Catalyst Synthesis

Zirconium hydroxide was prepared in a rather classical way starting from $ZrOCl_2$, $8H_2O$ (0.4 mol dm^{-3}) in aqueous solution. The precipitation occurred upon addition of a 28 wt.% ammonia solution up to a pH value equal to 10 under stirring for 20 min at room temperature. The gel was filtered, washed with distilled water up to complete elimination of chloride anion in the filtrate, and then dried at 120°C for 16 h. The zirconium hydroxide so obtained was then sulfated by contacting the powder with 15 cm^3 of 0.1 *M* sulfuric acid solution per gram of powder. The sample in suspension was stirred for 20 min at room temperature, filtered on a pyrex frit, and dried at 120°C for 16 h. Finally the sample was calcined under an air flow at 550°C for 2 h, a procedure shown previously to yield the most acidic sample (10–12).

2. Catalyst Characterization

The sample was characterized by the BET method (S = 80 $m^2\ g^{-1}$), chemical analysis (S content equal to 2 wt.%), and X-ray diffraction (tetragonal zirconia structure). Catalytic properties of the sample were observed to correspond to strong acidity since *n*-butane was isomerized in a flow microreactor (flow rate 2.2 $m^3\ h^{-1}$, 10% butane in nitrogen as carrier gas). For instance, at 200°C a conversion level of 18% was reached with 98% selectivity in 2-methylpropane.

For comparison a pure zirconia sample was prepared following the same procedure, obviously without addition of sulfuric acid solution but with calcination under an air flow at 550°C. The sample (monoclinic phase) was observed to be totally inactive for *n*-butane isomerization, even above 200°C.

3. Infrared Spectroscopy Measurements

Measurements were carried out on self-supported wafers prepared under 2×10^3 kPa pressure. Some spectra were recorded with the powdered samples diluted in KBr (1% dilution) in order to avoid the absorption saturation at low wavenumber values.

The self-supported wafers (12 mg/cm^2) were prepared with the powder calcined under flowing air at 550°C for 2 h and cooled to room temperature under ambient atmosphere, i.e., under ambient humidity. The wafers were then outgassed at a desired temperature for 2 h under a vacuum of 0.13 mPa. The adsorption of the different probe molecules was carried out as follows:

—Incremental and measured amounts of water were introduced into the infrared cell at room temperature up to saturation vapor pressure (2.4 kPa).

—D_2O (99.99% enrichment) and $H_2{}^{18}O$ (10% enrichment) increments were also introduced following the same procedure.

—Carbon monoxide was adsorbed at room temperature under 1.3 kPa pressure and then outgassed at the same temperature.

—Pyridine was adsorbed under its saturation vapor pressure for 2 h at 22°C and then outgassed for 2 h at a given temperature. Careful dehydration of pyridine before use was carried out using a zeolite trap.

—Butane was adsorbed under 0.7 kPa pressure at room temperature and further outgassed at the same temperature.

The IR spectra were recorded with a Brucker IFS48 FTIR spectometer usually with 500 scans. The reference gas was either nitrogen when the gaseous phase was evacuated or the gas phase itself when it was not evacuated.

III. RESULTS

Infrared spectra of the sample after drying at 120°C, calcination in flowing air, further rehydration under ambient atmosphere, and then outgassing at room temperature, 180°C, and 200°C are shown in Figs. 1 and 2.

1. Transformation of the Precursor

The spectrum of the precursor after drying at 120°C and rehydration in ambient air (Fig. 1a) is similar to that observed by Sohn and Kim (14) and exhibits four bands. It is assigned to bidentate SO_4^{2-} ion in C_{2v} symmetry with ν_3 at 1207, 1136, and 1053 cm^{-1} and ν_1 at 997 cm^{-1}. An additional broad and intense band at 3400 cm^{-1} corresponds to the stretching vibration ν_{OH} of hydroxyl groups

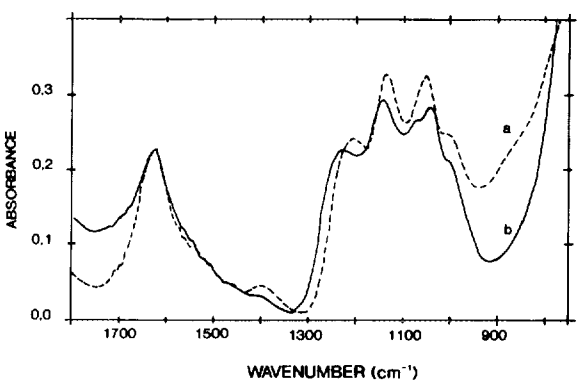

FIG. 1. Infrared spectra of sulfated zirconia in KBr wafer (1 wt.% dilution) after drying the precursor at 120°C in air and rehydration under ambient air at room temperature (spectrum a) and after calcination at 550°C under air flow and rehydration under ambient air at room temperature (spectrum b).

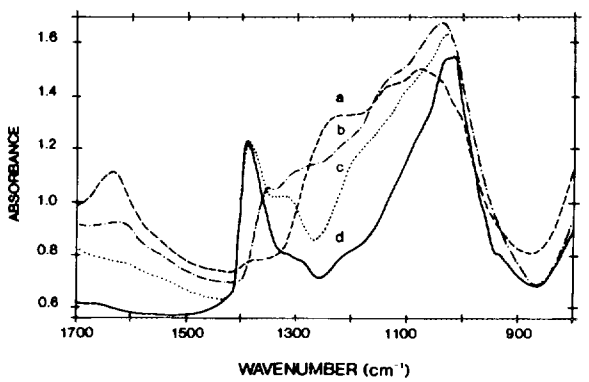

FIG. 2. Infrared spectra of a self-supported wafer of sulfated zirconia calcined at 550°C under air flow and rehydrated under ambient air at room temperature (spectrum a), and then outgassed at room temperature for 1 h (spectrum b), at 180°C for 1 h (spectrum c), and at 200°C for 1 h (spectrum d).

and adsorbed water accompanied by the 1628 cm^{-1} (δ_{HOH}) band.

Upon calcination at 550°C and rehydration in ambient air the spectrum (Fig. 1b) was slightly modified with an upward shift of the first two bands and the appearance of two shoulders at 1067 and 937 cm^{-1}. The 3400 cm^{-1} band intensity decreased strongly, while that at 1628 cm^{-1} varied slightly. Better resolved bands appeared clearly at 746, 557, 500, and 415 cm^{-1} characteristic of crystalline zirconia. It may thus be concluded that during calcination at 550°C condensation of the hydroxyl groups of $Zr(OH)_4$ occurred, leading to a crystallized sample without any change of the sulfated species.

2. *Outgassing of ZrO_2/SO_4^{2-}*

Outgassing at increasing temperature after calcination at 550°C and rehydration in air induced a progressive modification of the IR spectra (Figure 2). First, the ν_{OH} and δ_{HOH} vibrations of H_2O strongly decreased and disappeared at 180°C, while a band at 3645 cm^{-1} and a shoulder at 3570 cm^{-1} remained present, due to ν_{OH} of hydroxyl groups. As shown by the spectra of Fig. 3, these ν_{OH} are characteristic of the sulfated zirconia. Indeed, it is worthwhile noting that on nonsulfated zirconia two hydroxyl bands are observed at 3775 and 3665 cm^{-1} in agreement with previous work in the literature (15–19).

Second, new sulfate bands appeared near 1300 cm^{-1} and progressively shifted to 1393 cm^{-1}, while intensity in the 1200 cm^{-1} range decreased. At 180°C, the spectrum was composed of two bands of medium intensity and an intense band at 1387, 1320 cm^{-1}, and 1027 cm^{-1}, respectively, and a shoulder at 935 cm^{-1}. At 200°C, the intensity of the 1387 cm^{-1} band increased at the expense of the 1320 cm^{-1} one and shifted to 1393 cm^{-1}. Thereafter the spectrum did not vary up to 500°C.

It clearly appears that the bidendate SO_4^{-2} ion observed for the precursor was transformed by dehydration while its concentration did not change. Upon complete dehydration a species A was obtained with a characteristic band at 1387–1393 cm^{-1}. At an intermediate stage a species B characterized by the 1322 cm^{-1} band and a shoulder at 1200 cm^{-1} was obtained.

If outgassing was performed at 550°C, the spectrum was strongly modified with bands at 1293, 1183, 1083, 1046, and 1022 cm^{-1} and a threefold decrease in intensity. This clearly indicates that such outgassing at 550°C results in a decomposition of the sulfate species.

3. *Water Adsorption*

Incremental and known amounts of water were adsorbed on the sample calcined at 550°C under air flow and then outgassed in the IR cell at either 180 or 200°C for 1 h. H_2O, D_2O (99.99%), or $H_2{}^{18}O$ (10% enrichment) was introduced at room temperature. The spectra are given in Figs. 4 and 5. The following features may be noted as a function of water coverage.

—The 1387 cm^{-1} band decreased and shifted to 1322 cm^{-1} and then disappeared under water saturation.

—The intensity of the 1322 cm^{-1} band increased in a first stage and then disappeared under water saturation:

—The 1027 cm^{-1} band shifted to 1053 cm^{-1}, and shoulders appeared at 1076 and 1133 cm^{-1} and then at 1200 and 853 cm^{-1}.

For low H_2O coverage, a band was observed at 1680 cm^{-1}; it then vanished while a band near 1600 cm^{-1} appeared and increased proportionally to water coverage and shifted to 1634 cm^{-1} at water saturation. At the same time, broadening and shifting toward lower wavenumber values was observed for the band at 3645 cm^{-1}.

At water saturation for 15 min, the spectrum was identical to that obtained before outgassing.

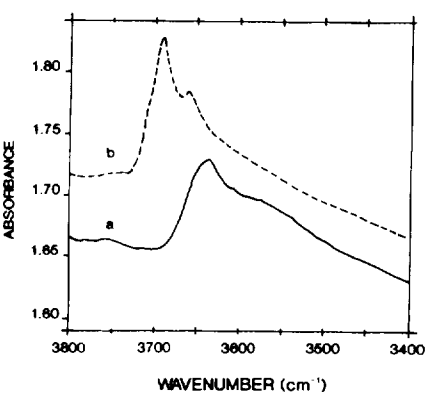

FIG. 3. Infrared spectra of self-supported wafer of sulfated zirconia calcined at 550°C under air flow and outgassed at 200°C for 1 h (spectrum a) and of pure zirconia treated under the same conditions (spectrum b).

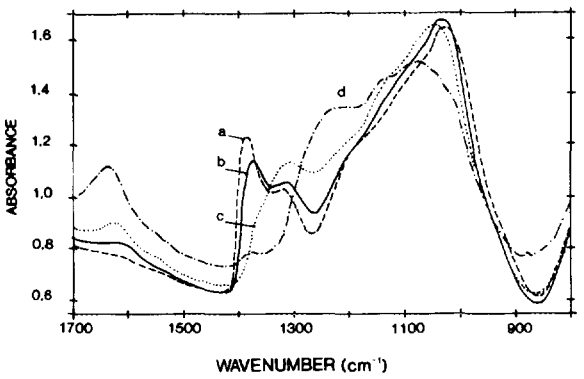

FIG. 4. Infrared spectra of self-supported wafer of sulfated zirconia calcined at 550°C under air flow and outgassed at 180°C for 1 h (spectrum a). Adsorption of water increments equal to $H_2O/S = 0.18$ (spectrum b), $H_2O/S = 0.36$ (spectrum c) and under partial pressure of water (0.7 kPa) at room temperature (spectrum d).

Upon desorption of adsorbed water, the first observation was a decrease in intensity of the 1073 and 1206 cm^{-1} bands in parallel with an increase of the 1322 and 1053 cm^{-1} bands. Second, the 1387 cm^{-1} band increased, while the 1322 and 1133 cm^{-1} bands decreased. Finally, at 180°C, the spectrum of the starting material was observed again.

D_2O was adsorbed on the sample desorbed at 200°C (Fig. 5). The same features as mentioned above were observed. However, the first D_2O increments, which were smaller than previously, allowed us to observe the progressive shift of the 1393 cm^{-1} band to 1368 and then to 1322 cm^{-1} and the presence of a small band at 1240 cm^{-1} related to the 1680 cm^{-1} one (1680/1240 = 1.35). Also for low coverage two bands were observed at 2696 and 2653 cm^{-1}. The wavenumber ratios 3645/2696 and 3575/2653 being equal to 1.35 allowed us to identify the bands to isotopic exchange of hydroxyl groups. At saturation an additional band at 1206 cm^{-1} was observed. It corresponds to the deformation vibration δ_{DOD} (1630/1206 = 1.35).

The adsorption of $H_2{}^{18}O$ on the sample finally outgassed at 200°C resulted in similar spectra to those observed for $H_2{}^{16}O$ adsorption. Thus either exchange with sulfate species did not occur or the ^{18}O labeling was too small (10%) to result in a detectable S=O vibration shift.

It is interesting to comment on the variations of intensity of the 1387 cm^{-1} band versus coverage. Straight lines are observed as shown in Fig. 6, regardless of whether H_2O, D_2O, or $H_2{}^{18}O$ adsorbate was used. Expressed as H_2O/S ratio it is notable that extrapolations to a nil optical density correspond to 0.65 and 0.9 for the 180 and 200°C outgassed samples, respectively. The extrapolated H_2O/S ratio values which tend toward 1 for outgassing temperature above 200°C lead us to suggest that the dehydrated sulfate species should adsorb one water molecule per surface sulfur atom and that almost all the sulfur atoms are accessible.

One finally distinguishes, in addition to the bidentate SO_4^{2-} observed upon water saturation, three different species with one of their characteristic bands at 1393–1387, 1368, and 1322 cm^{-1}, respectively. The first species transformed completely at low water coverage into the latter two species which disappeared upon water saturation. Such a transformation was observed to be reversible and in intermediate dehydration conditions (e.g., outgassing at 180°C) they all three coexisted in the sample.

In agreement with ab initio calculations (13), the spectrum observed after desorption at 200°C may be assigned to $(SO_3)_{ads}$. In the proposed model, the $(SO_3)_{ads}$ species is slightly pyramidized with three short S=O bonds (140 pm) and a long S—O bond (164 pm) and angles α and β between S=O bonds and S=O and S—O bonds respec-

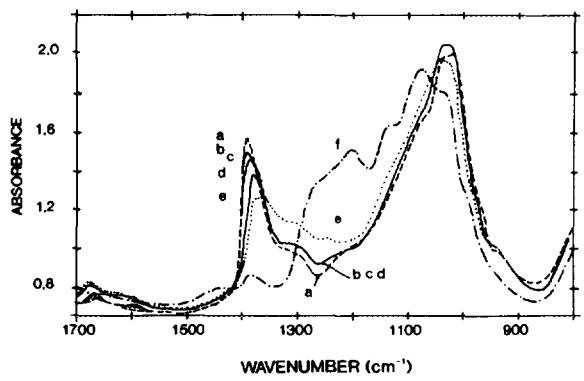

FIG. 5. Infrared spectra of self-supported wafer of sulfated zirconia prepared as in Fig. 4 but outgassed at 200°C for 1 h (spectrum a). Adsorption of D_2O increments equal to $D_2O/S = 0.05$ (spectrum b), $D_2O/S = 0.17$ (spectrum c), $D_2O/S = 0.29$ (spectrum d), $D_2O/S = 0.41$ (spectrum e) and under partial pressure of D_2O (0.7 kPa) at room temperature (spectrum f).

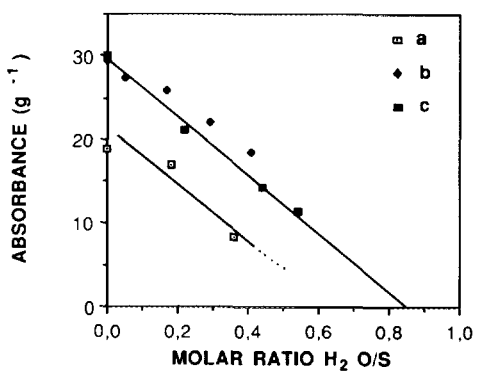

FIG. 6. Variations of the absorbance per gram of the 1393–1387 cm^{-1} IR bands versus the amount of water adsorbed using H_2O (a), D_2O (b), and $H_2{}^{18}O$ (c).

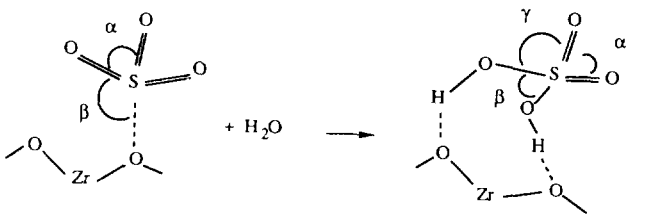

SCHEME 1

tively equal to 117 and 95°. As shown in Scheme 1, the symmetry of such a species is close to C_{3v}. Four stretching vibrations modes are expected to be active in infrared ($2A_1$ and $1E$). By analogy with the IR spectrum of gaseous SO_3 (20, 21), the absorption bands were assigned to vibration modes as reported in Table 1. Then applying the well known GF method (22) and assuming no interaction between stretching and bending modes the force constants were calculated and are also reported in Table 1. It is interesting to note that for the S=O bond the force constant is slightly inferior to that of gaseous SO_3 ($f = 10.6 \times 10^2$ N m^{-1}). This supports our suggestion that a dative interaction exists between the empty p orbital of SO_3 and the occupied orbital of O^{2-} ions on the surface.

It is suggested that in the presence of water the $(SO_3)_{ads}$ species were transformed into $(H_2SO_4)_{ads}$ species as described by Babou *et al.* (13). The model represented in Scheme 1 was characterized by 2 S=O bonds (140 pm), 2 S—O bonds (154 pm), and α, β, and γ angles equal respectively to 122, 100, and 109.6°. By analogy with the IR spectrum of gaseous H_2SO_4 (23, 24), the vibrations appearing upon water adsorption were assigned as reported in Table 2. The $\delta_{S—OH}$ bending expected near 1180 cm^{-1} was not detected due to the intensity of the stretching S—O bands; however, upon D_2O adsorption appearance of a weak absorption between 820 and 800 cm^{-1} may correspond to the $\delta_{S—OD}$ vibration.

Finally, the third species, characterized by the 1322 cm^{-1} band, could be $(HSO_4^-)_{ads}$ (25).

At low water coverage, the presence of the 1680 cm^{-1} band indicates the intermediate formation of H_3O^+,

TABLE 1

Vibration Modes and Force Constants for $(SO_3)_{ads}$

Vibration modes	Wavenumber (cm^{-1})	Force constants and interaction constants (10^2 N m^{-1})	Bond length (pm)
E: $(\nu_{S=O})_{as}$	1391	$f_1 = 10.22$	140
A_1: $(\nu_{S=O})_s$	1027	$f_1' = -0.37$	
A_1: $(\nu_{S—O})$	935	$f_2 = 5.80$	164
		$f_2' = 0.15$	

TABLE 2

Vibration Modes and Force Constants for $(H_2SO_4)_{ads}$

Vibration mode	Wavenumber (cm^{-1})	Force constants and interaction constants (10^2 N m^{-1})	Bond length (pm)
B_2: $(\nu_{S=O})_{as}$	1368	$f_1 = 9.68$	140
A_1: $(\nu_{S=O})_s$	1250	$f_1' = -0.36$	
B_1: $(\nu_{S—O})_{as}$	1040	$f_2 = 6.24$	154
A_1 $(\nu_{S—O})_s$	853	$f_2' = -0.22$	
		$f'' = -0.2$	

which at higher water coverage transforms into $(H_2O)_nH^+$. Several models have been proposed in the literature to explain the presence of a band at 1390 cm^{-1} for numerous sulfated oxides. If it is assumed that the high frequency characterizes a high covalency S=O vibrator, at least two attributions may be proposed. The first one, in agreement with the spectra of compounds such as XSO_2Y, assigns this band to the asymmetric stretching vibration of a $>SO_2$ group (8, 14, 26) and the other, on the basis of isotopic $^{16}O/^{18}O$ exchange, assigns it to a single $\equiv$S=O species (15, 16, 19).

4. *CO Adsorption*

No CO adsorption was observed on a sample outgassed at 180°C, but after outgassing at 350°C and subtracting the gaseous phase contribution the spectrum exhibited a narrow band at 2200 cm^{-1}, while the sulfate bond at 1393 cm^{-1} shifted to 1379 cm^{-1}. The initial spectrum was obtained again by desorption of CO at room temperature.

At variance with the data of Morterra *et al.* (19), shoulders at 2193 and 2182 cm^{-1} were not observed. These two latter bands have been assigned to CO adsorbed on coordinatively unsaturated Zr^{4+} cations of the bare oxide part not covered by sulfate species. As a matter of fact the amount of S in the present sample corresponds to total coverage of zirconia surface by a monolayer of sulfated species (10). It may thus be suggested that the 2200 cm^{-1} band corresponds very probably to CO adsorbed on the S^{6+} cation of the $(SO_3)_{ads}$ species. The shift and decrease in intensity of the 1393 cm^{-1} band may be interpreted as due to the above interaction since CO which is a weak base induces a weak electron transfer from sulfur to terminal oxygens, which decreases the S=O bond strength and thus its vibration frequency. This conclusion is in agreement with theoretical calculation (13) which showed that the OC–$(SO_3)_{ads}$ complex is unstable.

In intermediate dehydration conditions, the three species $(H_2SO_4)_{ads}$, $(HSO_4^-)_{ads}$, and $(SO_3)_{ads}$ coexist and one may suggest that CO can interact only with the Lewis

acid sites $(SO_3)_{ads}$ which are in too low amount to be detected.

5. *Pyridine Adsorption*

After contacting the sample outgassed at 200°C for 1 h with pyridine at room temperature for 15 min., outgassing was carried out at room temperature and at increasing temperatures up to 450°C for 2 h. The spectra are shown in Fig. 7.

Pure zirconia gives only pyridine species adsorbed on Lewis acid sites (designated L_1) with IR bands at 1444 and 1607 cm^{-1} (7, 27). Sulfated zirconia exhibited additional bands at 1459 and 1630 cm^{-1} assigned to new Lewis sites (designated L_2) and at 1542 and 1638 cm^{-1} assigned to Brønsted sites (designated B). The latter two sites L_2 and B are obviously related to the presence of sulfated species. The variations of the band intensities of the three pyridine species (L_1, L_2, and B) as a function of outgassing temperature are given in Fig. 8. It appears that L_2 sites are the strongest acid sites since their band intensity decreased less readily than the other ones.

It is worthwhile noting that Brønsted sites are unambiguously detected and are related to sulfate species. Such species are mentioned in some cases in the literature (10, 16, 17, 27, 28) but not in others (14, 15, 29). It is clear to us that this discrepancy arises only from the fact that such Brønsted sites are very sensitive to dehydration, i.e., to heat and vacuum treatment conditions before pyridine adsorption. Such a conclusion was also reached by Morterra *et al.* (19), who have shown that after desorption at 400°C no Brønsted sites were observed while they did reappear upon water adsorption.

The presence of L_1 Lewis sites has already been detected and assigned to coordinatively unsaturated Zr^{4+} ions, while L_2 Lewis sites have not yet been mentioned to our knowledge.

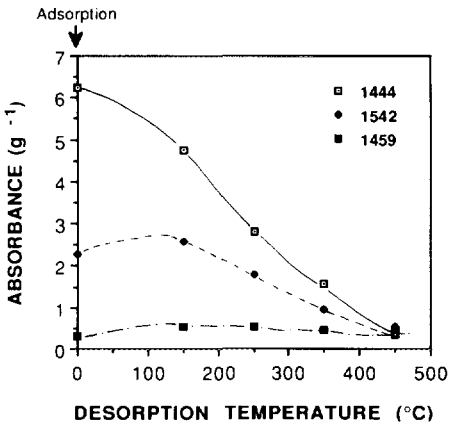

FIG. 8. Variations of intensities of the 1444 (L_1 site), 1459 (L_2 site), and 1542 cm^{-1} (B site) infrared bands versus outgassing temperatures for a self-supported wafer of sulfated zirconia outgassed at 200°C, contacted with pyridine at room temperature, and outgassed at increasing temperatures. ("Adsorption" designates the absorbance value before outgassing.)

Note that the species intensity of L_1 sites was much larger than that of L_2 sites by one order of magnitude. This seems to be contradictory to its assignment to Zr^{4+} cations on bare zirconia surface since the surface was suggested above to be completely covered by sulfated species (monolayer coverage). It is possible that the pyridinium ions formed weaken the bond between the sulfated species and the surface which then would become partly sulfate free. In fact, the bands of the sulfated species were deeply modified with a shift of the 1393 and 1027 cm^{-1} bands toward 1302 and 1050 cm^{-1}, respectively. By desorption a reversible and progressive displacement was observed (as shown in Fig. 9).

This effect is attributed to a weakening of the S=O bonds which may be induced by electron transfer from

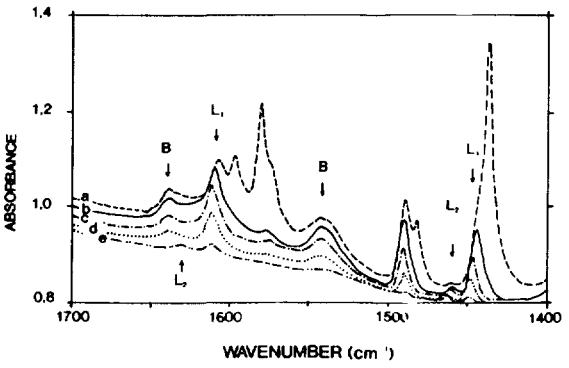

FIG. 7. Infrared spectra of pyridine adsorbed at room temperature under its partial pressure (spectrum a) and outgassed at room temperature (spectrum b), at 150°C (spectrum c), at 250°C (spectrum d), and at 450°C (spectrum e).

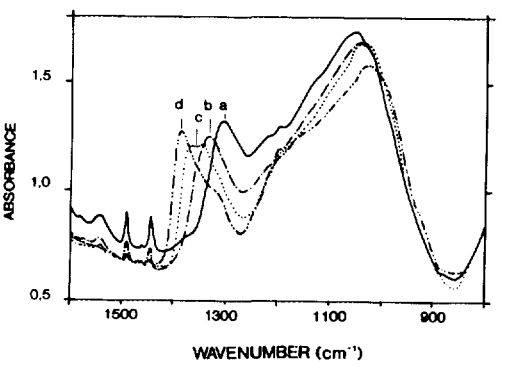

FIG. 9. Modifications of the sulfated IR bands upon pyridine adsorption on the sample and under conditions described in the caption to Fig. 7, pyridine being desorbed at room temperature (spectrum a), 150°C (spectrum b), 250°C (spectrum c), and 450°C (spectrum d).

the pyridine molecule (strong base) toward a Zr^{4+} cation (Lewis acid site) (10) or by direct interaction of the pyridine molecule with the sulfated species as suggested by Komarov and Sinilo (17).

As shown above, three species coexist at the surface of sulfated zirconia dehydrated at 180°C. Interaction of pyridine (Py) with these species may be described as follows:

$$(SO_3)_{ads} + Py \rightarrow (SO_3\ Py)_{ads}$$

$$(H_2SO_4)_{ads} + Py \leftrightharpoons (HSO_4^-)_{ads} + PyH^+$$

$$(HSO_4^-)_{ads} + Py \leftrightharpoons (SO_4^{2-})_{ads} + PyH^+$$

and

$$(H_3O^+)_{ads} + Py \leftrightharpoons PyH^+ + H_2O$$

The first reaction corresponds to the formation of L_2 species and the latter three to the formation of B species. As for water adsorption these latter reactions are equilibrated and are strongly displaced toward the right since pyridine is a very strong base. Moreover, one may suggest that the formation of (SO_4^{2-}) species induced an uncovering of the Zr^{4+} ions able to form L_1 species with pyridine.

6. *Butane Adsorption*

Butane can be considered as a very weak base (weaker than CO) and should therefore be adsorbed only on very strong acid sites. Upon adsorption at room temperature a shift of the ν_{CH} toward lower frequency values with respect to gaseous butane spectrum was observed with the disappearance of rotational bands and an increase of the 2870 cm^{-1} band as shown in Fig. 10. Two small bands at 1466 and 1384 cm^{-1} may be assigned to deformation vibrations δ_{CH_2} and δ_{CH_3}. Thus the adsorbed butane has lost some of its degrees of freedom but it interacts very weakly with the surface since the IR bands of sulfated species were not shifted appreciably and the butane spectrum disappeared upon outgassing at room temperature.

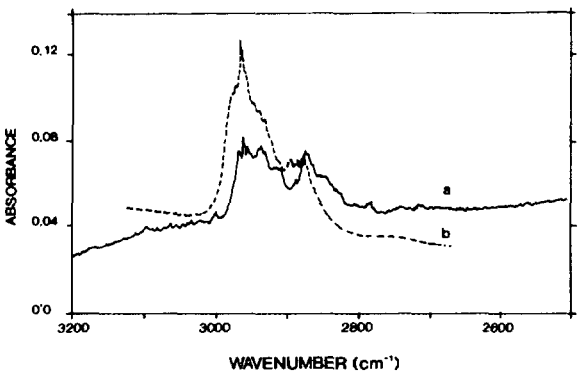

FIG. 10. Infrared spectra of butane adsorbed at room temperature on the sulfated zirconia sample outgassed at 200°C for 1 h after the usual activation procedure and after subtraction of the gaseous phase (spectrum a). Gaseous *n*-butane (spectrum b).

IV. DISCUSSION

It clearly appears from the experimental data given above that there is a reversible effect of water on the sulfated species on the surface of zirconia. One may consider the equilibria of ionization and dehydration of adsorbed sulfuric acid

$$(SO_3)_{ads} + (H_2O)_{ads} \leftrightharpoons (H_2SO_4)_{ads}$$

$$(H_2SO_4)_{ads} + (H_2O)_{ads} \leftrightharpoons (H_3O^+)_{ads} + (HSO_4^-)_{ads}$$

$$(HSO_4^-)_{ads} + (H_2O)_{ads} \leftrightharpoons (H_3O^+)_{ads} + (SO_4^{2-})_{ads}$$

with the following assignments for the different species:

bidendate $(SO_4^{2-})_{ads}$: ν_3 bands at 1207, 1136, and 1053 cm^{-1}
ν_1 band at 997 cm^{-1}.
$(H_3O^+)_{ads}$: 1680 cm^{-1}
$(HSO_4^-)_{ads}$: 1322, shoulder at 1200 cm^{-1}.
$(H_2SO_4)_{ads}$: 1368, 1250, 1040, and 853 cm^{-1}
$(SO_3)_{ads}$: 1387–1393, 1027, and 953 cm^{-1}.

One may then imagine that sulfation of zirconium hydroxide occurs according to the following scheme. In the aqueous impregnation solution, H_2SO_4 is totally ionized according to

$$H_2SO_4 \rightleftharpoons SO_4^{2-} + 2H^+$$

and the zirconium hydroxide surface traps the protons as follows:

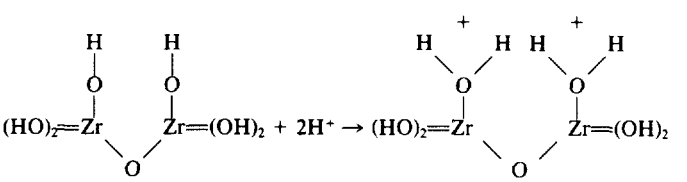

In such a representation, only the four valence bonds and not the four dative bonds are considered, as distinct from the scheme of Babou *et al.* (13) which takes all eight bonds into account.

The SO_4^{2-} anions being trapped on this ionized surface, the ionization equilibrium is shifted to the right. Calcination at 550°C produces condensation of hydroxyl groups which transforms zirconium hydroxide into zirconia. In

the presence of moisture the sulfate species remain solvated and the effect of further dehydration can be represented as follows:

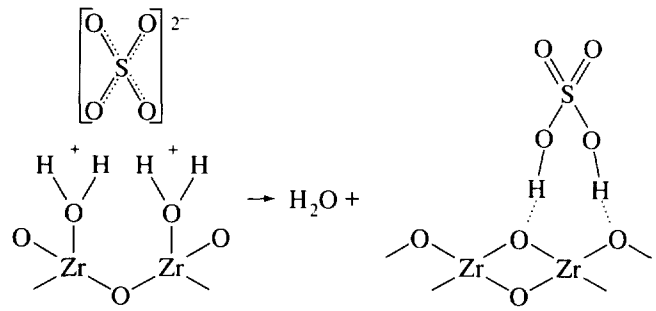

Desorption at room temperature shifts the equilibrium to the right and desorption above 200°C liberates a second water molecule with formation of $(SO_3)_{ads}$ linked by dative bonds whose stability is established by the amphoteric characters of the Lewis acid and base, SO_3 and ZrO_2, respectively.

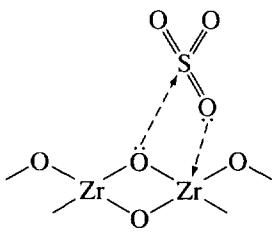

Such a model is based on quantum chemistry calculations as described in Ref. (13). This shows that in fact sulfated zirconia may tentatively be considered as a sulfuric acid molecule grafted at the surface of zirconia in a state very sensitive to dehydration in a reversible manner. At high dehydration conditions (e.g., outgassing above 200°C) one obtains $(SO_3)_{ads}$ species which exhibit strong Lewis properties, as evidenced previously (11), able to ionize a benzene molecule (ionization potential = 9.25 eV) into a $C_6H_6^+$ radical cation. At intermediate dehydration degrees (e.g., in a 180–200°C range under vacuum) H_3O^+ and HSO_4^- species induce a very strong Brønsted acidity. Such an acidity was shown by theoretical calculations given in Ref. (13) to be close to that of sulfuric acid, i.e., to be strongly acidic but not really superacidic.

The reversible effect of water is particularly important for catalytic applications. As a matter of fact, using dried butane results in a decrease in catalytic activity for *n*-butane isomerization and vice versa when a low amount of water is added. This effect is to be compared with the classic Friedel–Crafts type of reaction known for a long time to necessitate a very low amount of water in the feed to be effective (1, 30). This also shows how delicate it is to define the experimental conditions of catalyst activation to obtain this grafted sulfuric acid species and establish catalytic reaction conditions to obtain and maintain good catalytic performances.

A question which obviously arises is why zirconia supports appear to be particularly efficient for grafting strongly acidic sulfuric acid molecules while other supports such as Al_2O_3, TiO_2, and HfO_2 are not so efficient (26). It is striking that the positive charge borne by the Zr^{4+} cation seems particularly well fitted to result in high Lewis acidity transferable to adsorbed sulfate species. A rough calculation of the charge borne by the cation has been performed using a simplified version of Mortier's formula (31) based on Sanderson's electronegativity approach

$$q_i = \frac{(\chi - \chi_i)}{1.36\sqrt{\chi_i}} \quad \text{with } \chi = \frac{\sum_{i=1}^{n} p_i\sqrt{\chi_i} + 1.36Z}{\sum_{i=1}^{n} p_i \frac{p_i}{\sqrt{\chi_i}}},$$

where χ_i is Pauling's electronegativity for atom i, n_i is the stoichiometry in atom i, χ is the electronegativity of the ensemble, and Z is the charge of the ensemble.

It turns out that one obtains 0.78, 0.60, and 0.51 for ZrO_2, Al_2O_3, and Fe_2O_3, respectively, in reasonable agreement with the acidity strength as determined from catalytic reaction testing (26, 32, 33).

REFERENCES

1. See, for instance, Pines, H., "The Chemistry of Catalytic Hydrocarbons Conversion." Academic Press, New York, 1981.
2. Corma, A., and Martinez, A., *Catal. Rev. Sci. Eng.* **35,** 483 (1993).
3. Corma, A., Juan-Rajadell, M. I., Lopez-Nicto, J. M., and Martinez, A., *Appl. Catal. A* **111,** 175 (1994).
4. Yamaguchi, T., Nakano, Y., and Tanabe, K., *Bull. Chem. Soc. Jpn.*, 51 (1978).
5. Hino, M., and Arata, K., *Chem. Lett.*, 1259 (1979).
6. Tanabe, K., Kayo, A., and Yamaguchi, T., *J. Chem. Soc. Chem. Commun.*, 602 (1981).
7. Kayo, A., Yamaguchi, T., and Tanabe, K., *J. Catal.* **83,** 99 (1983).
8. Yamaguchi, T., Jin, T., Ishida, I., and Tanabe, K., *Mater. Chem. Phys.* **17,** 3 (1986).
9. Arata, K., and Hino, H., *Appl. Catal.* **59,** 197 (1990).
10. Nascimento, P., Akratopoulou, C., Oszagyan, M., Coudurier, G., Travers, C., Joly, J. F., and Védrine, J. C., *in* "Proceedings, 10th International Congress on Catalysis, Budapest, 1992" (L. Guczi, F. Solymosi, and P. Tétényi, Eds.), p. 1185. Akadémiai Kiadó, Budapest, 1993.
11. Chen, F. R., Coudurier, G., Joly, J. F., and Védrine, J. C., *J. Catal.* **143,** 616 (1993).
12. Babou, F., Bigot, B., Coudurier, G., Sautet, P., and Védrine, J. C., *in* "Acid–Base Catalysis II" (H. Hattori, M. Misono, and Y. Ono, Ed.), *Stud. in Surf. Sci., Ser.*, **90,** 519, Elsevier, Amsterdam, 1994.
13. Babou, F., Sautet, P., and Bigot, B., *J. Phys. Chem.* **97,** 11501 (1993).
14. Sohn, J. R., and Kim, H. J., *J. Mol. Catal.* **52,** 379 (1989).
15. Bensitel, M., Saur, O., and Lavalley, J. C., *Mater. Chem. Phys.* **17,** 249 (1987).
16. Waquif, M., Bachelier, J., Saur, O., and Lavalley, J. C., *J. Mol. Catal.* **72,** 127 (1992).
17. Komarov, V. S., and Sinilo, M. F., *Kinet. Katal.* **29,** 701 (1988).

18. Agron, P. A., Fuller, E. L., and Holmes, H. F., *J. Colloid Interface Sci.* **52,** 553 (1975).
19. Morterra, C., Aschieri, R., and Volante, M., *Mater. Chem. Phys.* **20,** 539 (1988).
20. Lovejoy, R. W., Colwell, J. H., Eggen, P. F., and Halsey, G. D. *J. Chem. Phys.* **36,** 612 (1962).
21. Bent, B., and Ladner, W. R., *Spectrochim. Acta* **19,** 931 (1962).
22. Wilson, E. B., Decius, J. C., and Cross, P. C., "Molecular Vibrations." McGraw–Hill, New York, 1955.
23. Chackalackal, S., and Stafford, F. E., *J. Am. Chem. Soc.* **88,** 723 (1966).
24. Giguère, G., and Savoie, R., *Can. J. Chem.* **41,** 287 (1963).
25. Gillespie, R. J., and Robinson, E. A., *Can. J. Chem.* **40,** 644 (1986).
26. Jin, T., Yamaguchi, T., and Tanabe, K., *J. Phys. Chem.* **90,** 4794 (1986).
27. Nakano, Y., Iizuka, T., Hattori, H., and Tanabe, K., *J. Catal.* **57,** 1 (1979).
28. Hino, H., and Arata, K., *J. Chem. Soc. Chem. Comm.*, 851 (1980).
29. Tret'yakov, N. E., Pozdnyakov,D. V., Orenskaya, O. M., and Filimonov, V. N., *Zh. Fiz. Khim.* **44,** 596 (1970).
30. Kramer, G. M., Skomoroski, R. M., and Hinlicky, J. A., *J. Org. Chem.* **28,** 1029 (1963).
31. Henry, M., Ph.D. thesis, University of Paris VI, 1988.
32. Babou, F., Coudurier, G., and Védrine, J. C., *J. Chim. Phys.*, in press.
33. Babou, F., Ph.D. thesis, University of Lyon No. 88 94 (1994).